MODELLING PLOUGHING AND CUTTING PROCESSES IN SOILS

J. P. Hambleton[1], S. A. Stanier[2], D. J. White[2] and S. W. Sloan[1]
[1]*ARC Centre of Excellence for Geotechnical Science and Engineering, The University of Newcastle, Callaghan, NSW, Australia*
[2]*ARC Centre of Excellence for Geotechnical Science and Engineering, The University of Western Australia, Crawley, WA, Australia*

ABSTRACT

Economic growth in Australia and the rest of the world is linked to the scale of construction and mining, and the amount of earth moved each year in these operations is difficult to fathom. When distributed evenly across the world's population, each individual moves several tonnes of earth each year. This paper highlights current and future research initiatives within the ARC Centre of Excellence for Geotechnical Science and Engineering (CGSE) aimed at developing rigorous, mechanics-based models for fundamental ploughing and cutting processes in soils. State-of-the-art physical modelling is integrated with the development of new techniques for analytical and numerical modelling to elucidate and predict the full progression of forces and deformations in both two-dimensional and three-dimensional processes. A new analytical model for cutting in dry sand is presented, and preliminary results from numerical and physical modelling are described. The analyses reveal effects that available models fail to consider and illustrate how the development of rigorous models may facilitate improvements in production and efficiency in earthmoving operations.

1 INTRODUCTION

Technological demands associated with human activity often outstrip scientific understanding, and few areas are as striking in this respect as the mechanics of earthmoving. Earthmoving processes are ubiquitous in the natural and man-made environments (Figure 1), and they appear over scales ranging from millimetres (e.g., asperity interaction at contact interfaces) to kilometres (e.g., folding and faulting of the earth's crust). The magnitude of earthmoving operations is staggering. Two decades ago, Hooke (1994) estimated that between 30 and 35 billion tonnes of earth are moved annually worldwide for housing excavations, mineral production, and road building. This figure corresponds to 6 tonnes annually per capita worldwide, and will have risen sharply over the past 20 years due to the rise in construction and mining associated with economic development (Hooke, 2000). In Australia, the mining industry alone contributed nearly 8% to the nation's total Gross Value Added, or $96 billion, from 2010 to 2011 (Australian Bureau of Statistics, 2011). BHP Billiton alone has exported more than one billion tonnes of Australian iron ore from the Pilbara since 1966.

Whether the application is civil construction, mining, tribology, or even planetary exploration (Wilkinson and DeGennaro, 2007), the means by which earth is mechanically moved and shaped often comes down to two fundamental processes: ploughing and cutting. Both terms refer to the progressive displacement of relatively large volumes of earth by a tool or object, and the difference lies in whether material is subsequently removed, as illustrated in Figure 2. From an engineering perspective, understanding the full history of material deformation is essential for prediction of the required forces and therefore machinery capabilities. In soil-machine interaction, one typically wishes to minimise tool forces for optimal machine performance. Alternatively, tractive devices such as grousers (Sutoh *et al*., 2013) and grillage foundations (Knappett *et al*., 2012) are designed to maximise resistance (Figure 1c).

From a theoretical viewpoint, ploughing and cutting processes pose tremendously challenging problems involving unsteady plastic flow, often three-dimensional deformation (Figure 1b), contact interaction, material instabilities, and rate effects from inertial forces and hydro-mechanical coupling (for saturated or partially saturated media). Astonishingly, the predominant models for ploughing and cutting in soils rest on methods dating back to the eighteenth century. Synthesis of review papers and monographs (e.g., Balovnev, 1983; McKyes, 1985; Godwin and O'Dogherty, 2007) reveals a strong dependence on empirical relationships and crude models subsumed from theories developed for retaining walls and foundations, although more developed theories can be found in the metalworking and tribology literature (Atkins, 2009). Current models do not consider the full, unsteady process of deformation, thus they neglect potentially significant effects arising from accumulation of soil and the evolution of material strength with plastic strain. Narrow objects and tools pose a special challenge in light of the fundamentally three-dimensional pattern of deformation induced, and no general framework for analysis has been developed (Godwin and O'Dogherty, 2007).

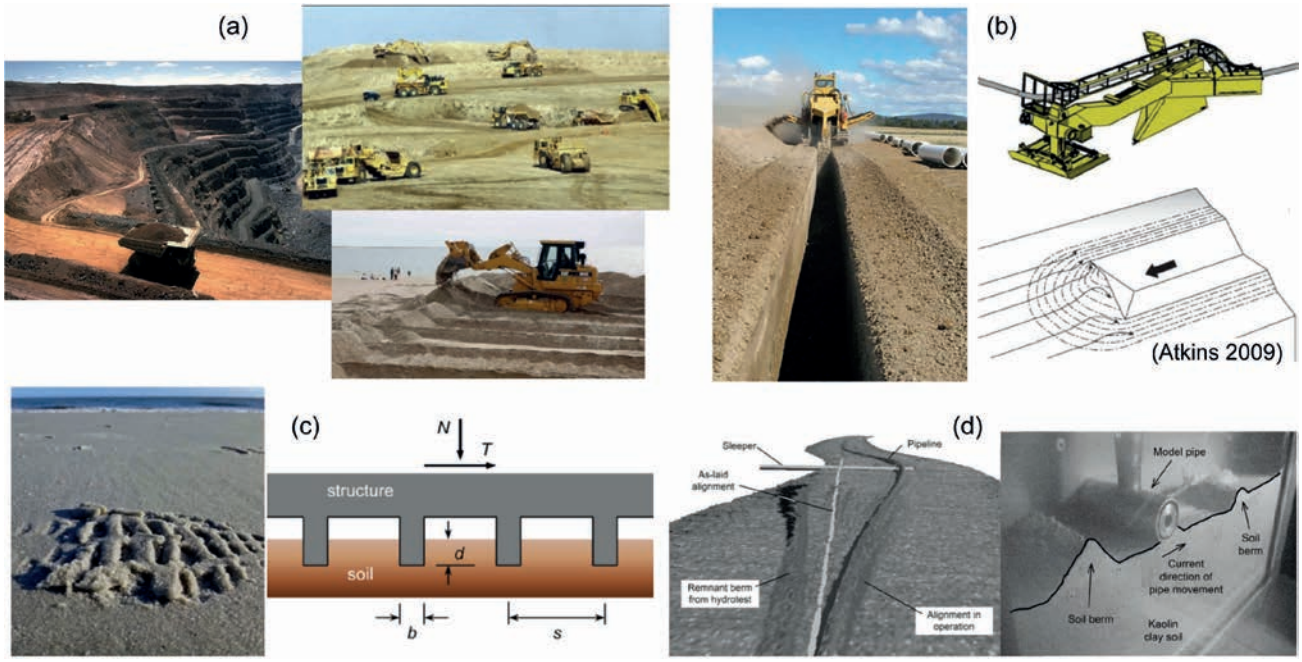

Figure 1: Examples of earthmoving processes in soils: (a) civil construction and mining; (b) trenching and ploughing for burial of pipelines and cables; (c) tractive devices; (d) lateral buckling of pipelines (cf. White and Dingle, 2011).

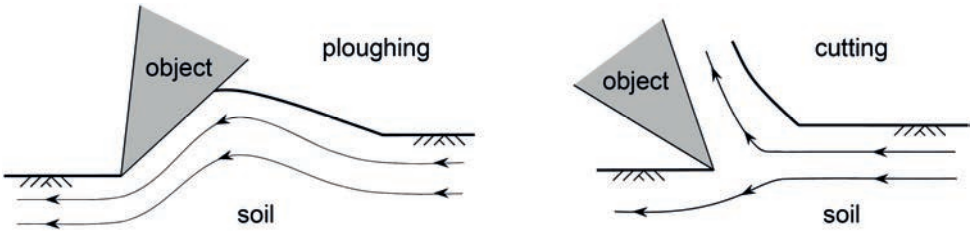

Figure 2: Ploughing and cutting processes in soils.

The overarching goal of current and future research initiatives within the ARC Centre of Excellence for Geotechnical Science and Engineering (CGSE) is to develop rigorous, mechanics-based models for fundamental ploughing and cutting processes in soils. Specific aims are as follows:

1. To quantify, precisely and definitively, the complete history of forces and deformation occurring in *two-dimensional* (plane strain) ploughing and cutting processes with characteristic geometries.
2. To evaluate force histories and, using suitable visualisation techniques, deformation histories for *three-dimensional* ploughing and cutting processes with characteristic geometries.
3. To understand variations in behaviour occurring over a full range of physical scales, until now largely neglected (Atkins, 2009; Palmer, 1999), and establish suitable scaling relationships.
4. To devise bespoke, robust, efficient, and flexible computational approaches that are motivated and fully validated by experimental results obtained in (1)-(3) and can accurately model two-dimensional and three-dimensional ploughing and cutting processes for application in engineering practice, in order to improve the design of earthmoving processes and earthmoving machinery.

This paper focuses mainly on two-dimensional analytical and numerical modelling (Item 4), with preliminary results from 1g physical modelling (Item 1) presented for partial validation. Section 2 presents a new analytical model for cutting in dry sand by a flat, vertical blade (tool) undergoing simple lateral motion. Sections 3 and 4 provide overviews of numerical and physical modelling, respectively, and comparisons between theoretical predictions and preliminary experimental results.

2 APPROXIMATE ANALYTICAL MODELLING

While analytical models for modelling ploughing and cutting processes in soils have existed for decades (cf. McKyes, 1985; Godwin and O'Dogherty, 2007), these models universally neglect the full process of deformation. In particular, available models either ignore the accumulation (accretion) of material ahead of the tool or replace this material with an equivalent surcharge, in much the same way that Terzaghi (1943) regarded the effect of soil above a footing's depth of embedment. Both approaches fail to consider the full complexity of ploughing and cutting processes as moving boundary value problems, wherein the shape of the free surface is unknown beforehand. This paper presents an analytical model that is highly simplified yet complete in its treatment of the full process of deformation as a moving boundary value problem. The analysis demonstrates one of several potential pitfalls of the conventional modelling assumptions.

Figure 3 depicts the approximate analytical model for the cutting process in dry sand. For simplicity, the cutting tool is taken to be a thin, vertical blade. The tool is initially placed at penetration depth δ within the sand and then moves laterally at constant penetration depth. The width of the blade is considered to be much greater than the penetration depth, such that plane-strain (two-dimensional) conditions prevail. It is assumed that the material obeys the Mohr-Coulomb yield criterion, and the key material parameters are thus the angle of internal friction ϕ and unit weight γ. At the tool-sand interface, dry friction characterised by wall friction angle ϕ_w is assumed, where $0 \leq \phi_w \leq \phi$. Rate effects are deemed of secondary importance (cf. Balovnev, 1983), and the process is considered to be quasi-static. The model rests on three major assumptions regarding the mode of deformation within the soil:

1. All deformation is taken to occur along a single, straight slip surface that extends from the tip of the tool towards the soil surface at some unknown inclination angle β (Figure 3a).
2. The unknown free surface, which generally varies in shape and location as a result of material accumulation, is approximated by a straight line (Figure 3a).
3. Potential volume change within the material (densification or dilatancy) is neglected.

Based on the above assumptions, the following expression for the lateral force P can be derived considering equilibrium and the requirement that stresses (and force resultants) on the slip surface must satisfy the Mohr-Coulomb failure criterion:

$$P = W \frac{\tan\left(\beta + \phi\right)}{1 - \tan\phi_w \tan\left(\beta + \phi\right)} \tag{1}$$

In Equation (1), W is the weight of material above the slip surface (see Figure 3a) calculated as:

$$W = \frac{\gamma \delta h}{2 \tan\beta} \tag{2}$$

Equations (1) and (2) contain two unknowns. The first is the inclination angle of the slip surface β. This angle is conventionally determined based on minimisation of the force P, often by analogy to Coulomb's theory of passive earth pressure (e.g., McKyes, 1985; Godwin and O'Dogherty, 2007; Knappett *et al.,* 2012). The underlying assumption is that the mode of deformation requiring the least force is the one most likely to occur. This "principal of minimum effort" has also been proposed as a potential explanation for the preferential appearance of a particular displacement field in steady plastic flow (Hill, 1950; Petryk, 1979), where numerous admissible displacement fields often exist. For the problem at hand, the angle β that minimises P, denoted by β_{opt}, is readily obtained by solving $\partial P/\partial\beta = 0$

$$\tan\beta_{opt} = \frac{2\sin\phi\left(\cos\phi - \tan\phi_w \sin\phi\right)}{1 - \cos 2\phi + \tan\phi_w \sin 2\phi + 2\sqrt{\sin\phi\left(\tan\phi_w \cos\phi + \sin\phi\right)}} \tag{3}$$

The second unknown in Equations (1) and (2), the height of accumulated matieral h, can be assessed by considering mass balance. In accordance with the third assumption listed above, mass balance and volume (area) balance are equivalent, and any increase in the volume of accumulated material ΔV is equal to the volume displaced by the tool ΔV_0, as depicted in Figure 3b. Upon equating the total volumes, $V = V_0$, one arrives at the following expression for h:

$$h = 2u \tan\beta + \delta \tag{4}$$

where u is the total tool displacement.

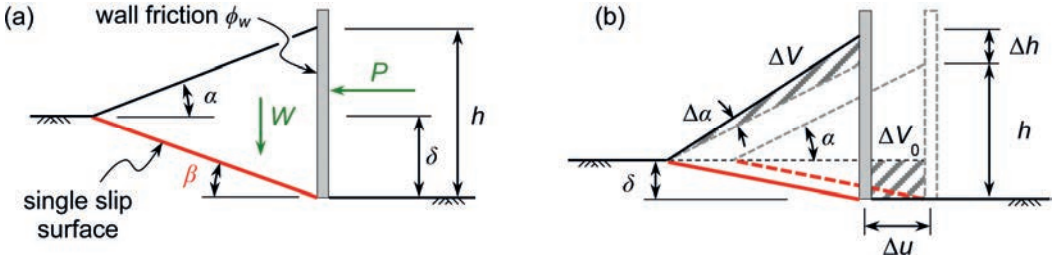

Figure 3: Analytical model for cutting in dry sand: (a) assumed mode of deformation and (b) incremental displacement of soil corresponding to an increment of tool displacement Δu for constant β

Equations (1)-(4) can be combined to give the following relationship between the normalised force $P/\gamma\delta^2$ and the normalised tool displacement u/δ for given parameters ϕ and ϕ_w:

$$\frac{P}{\gamma\delta^2} = \left(2\frac{u}{\delta}\tan\beta_{opt} + 1\right)\frac{\tan\left(\beta_{opt}+\phi\right)}{2\tan\beta_{opt}\left[1-\tan\phi_w\tan\left(\beta_{opt}+\phi\right)\right]} \tag{5}$$

While Equation (5) may at first seem like a reasonable solution, a salient issue arises when one considers relatively large values of tool displacement. As shown in Figure 3b, the inclination angle of the free surface, denoted by α, exhibits unrestricted growth leading eventually to avalanching of the material (i.e., slope failure). Equation (5) is therefore plausible as a force-displacement history only for relatively small displacements.

An alternative and somewhat indirect method for determining β is to postulate that avalanching occurs continuously throughout the process of deformation. Taking the friction angle ϕ as the angle of repose, this assumption imposes the condition $\alpha = \phi$, from which the following alternative to Equation (3) can be derived:

$$\tan\beta_{aval} = \sqrt{\frac{1}{2}\frac{\delta}{u}\tan\phi} \tag{6}$$

where β_{aval} denotes the angle β obtained based on the assumption of continuous avalanching. In contrast to β_{opt}, which remains constant irrespective of the normalised displacement u/δ, the inclination angle β_{aval} changes, varying from $\beta_{aval} = 90°$ at $u/\delta = 0$ to $\beta_{aval} = 0$ as $u/\delta \to \infty$. Whereas the solution based on force minimisation ($\beta = \beta_{opt}$) leads to excessive values of slope angle α for large values of u/δ, the solution based on continuous avalanching ($\beta = \beta_{aval}$) becomes undefined for small values of u/δ.

Figure 4a shows examples of the normalised force-displacement histories predicted based on the analytical model with the two different approaches for determining β. A remarkable feature of Fig. 4a is that the curves corresponding to $\beta = \beta_{opt}$ and $\beta = \beta_{aval}$ intersect at some value of displacement. This implies that the force obtained under the assumption of continuous avalanching is in fact less than that predicted by minimisation for large values of displacement, thus posing an apparent contradiction. The contradiction reveals a basic flaw in conventional theories for ploughing and cutting, and it can be explained by the appearance of the variable h in Equation (2). In keeping with available models, which most commonly replace the accumulated material by an equivalent surcharge, h was initially regarded as an independent variable when minimising the force P to obtain β_{opt} (Equation (3)). As an independent parameter, h clearly cannot be determined through minimisation, since the force P simply drops to zero as the height h is reduced. However, inspection of Equation (4) reveals that h also depends on β, a fact that was neglected in the minimisation process. This suggests that yet another solution can be obtained by combining Equations (1), (2), and (4) and minimising the resulting expression. This third approach yields force-displacement histories that smoothly follow the trends depicted in Figure 4b, which were obtained simply by taking the smaller of the forces predicted by $\beta = \beta_{opt}$ and $\beta = \beta_{aval}$.

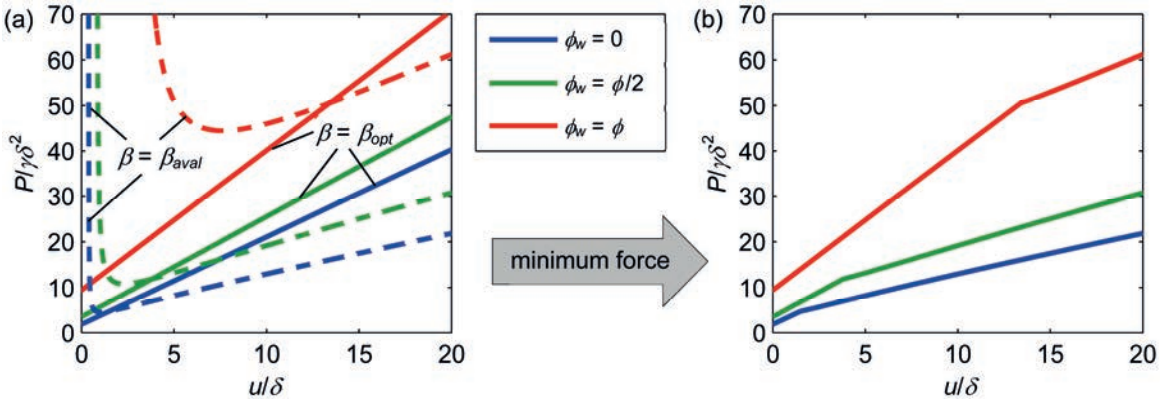

Figure 4: Force-displacement histories predicted by the analytical model for ϕ = 35° and differing values of wall friction angle ϕ_w: (a) solutions corresponding to force minimisation ($\beta = \beta_{opt}$) and continuous avalanching ($\beta = \beta_{aval}$); (b) composite curves obtained by considering overall minimum force.

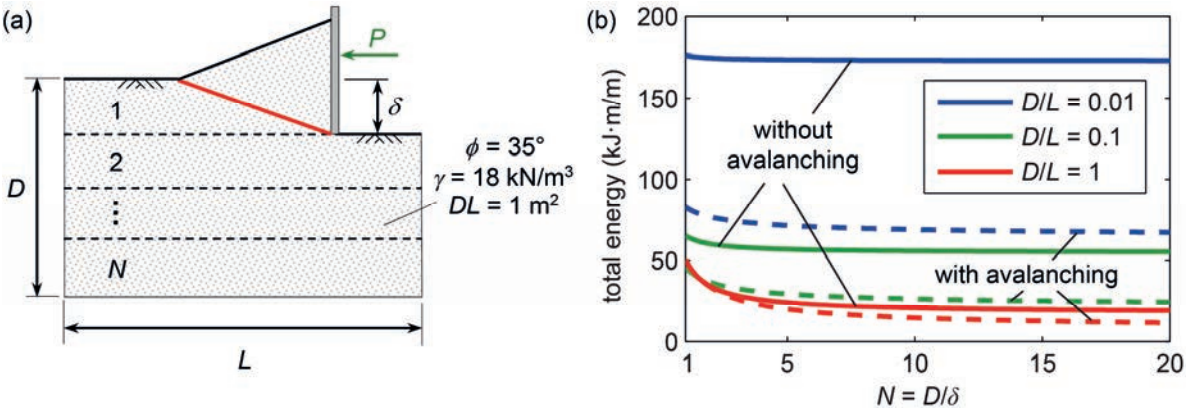

Figure 5: An example consisting of (a) excavation of a rectangular volume (area) of material in N layers and (b) the total required energy predicted by the proposed analytical model as a function of N and the normalised depth D/L.

The trends shown in Fig. 4b suggest that the rate of increase of the force diminishes as the displacement increases. From a practical viewpoint, this indicates that it may require less effort to excavate material in multiple thin layers rather than a single thick layer. To demonstrate this, Figure 5 explores how much energy is required to excavate a rectangular region of depth D and length L by removing the material in N layers, where $N = D/\delta$. The example considers the variation in total energy, computed as $E = N\int P du$ ($0 \le u \le L$), as a function of the number of layers N and the aspect ratio D/L. A total volume (area) of DL = 1 m^2 and a perfectly smooth blade ($\phi_w = 0$) are assumed. Figure 5b shows that the total required energy decreases as the number of layers N increases, and that the effect becomes much more pronounced as the depth of excavation D/L increases. Moreover, the results indicate that avalanching, which leads to lower force at large displacements compared to the conventional optimisation-based solution, dramatically reduces the predicted energy requirements.

3 NUMERICAL MODELLING

While analytical solutions of the type described in the previous section can deliver convenient expressions and clear physical insights, they are incapable of faithfully reproducing some of the effects observed in experiments and field tests. As explicit examples, two shortcomings of the model described in the previous section are (1) the potential oversimplification of assumed kinematics, especially with respect to the assumed failure mechanism and the shape of the free surface and (2) an assumed material model that is also potentially overly simplistic. This section describes a computational approach for modelling two-dimensional ploughing and cutting processes which can be used to overcome these and other issues.

In general terms, the proposed computational approach consists of first evaluating the displacement field within an increment of deformation based on the kinematic method of plasticity theory (cf. Chen, 1975) and then updating the deformed configuration based on the optimal incremental displacement field. The full process of deformation is thus modelled sequentially over a number of discrete displacement increments Δu. As a general technique, the concept was first implemented by Yang (1993) for steel-framed structures. More recently, Cubas *et al*. (2008) employed a similar

notion to model geological processes involving crustal folding and faulting, and Hambleton and Drescher (2012) successfully used the concept to model analytically the indentation processes in soils.

Figure 6 depicts one of the simplest possible implementations of the computational technique (Kashizadeh *et al,*. 2014), which can be regarded as an extension of the analytical model described in Section 2. The mode of deformation within an increment (Figure 6a) is identical to the one assumed in the analytical model (Figure 3a), except that the material surface is now discretised (Figure 6b), and the set of potential slip lines is constructed as the series of lines spanning between the nodes and the tip of the tool, each of which corresponds to a different value of β. The process of minimisation and sequential updating is shown in Figure 6b. Within each increment, an optimisation procedure is used to determine the angle β_{opt} that minimises the force P. The force P is again calculated using Equation (1). However, the weight W is now computed based on numerical integration rather than Equation (2). Once β_{opt} is determined through numerical minimisation, the deformed configuration is updated as shown in Figure 6b by updating the nodal coordinates.

Two key differences between the analytical and the numerical model are as follows. First, avalanching is considered on a local rather than a global level, and a dedicated subroutine operating with respect to the nodal points is implemented to predict and account for these local instabilities. For brevity, this subroutine is not described here; see Kashizadeh *et al*. (2014). The second major difference is the introduction of a softening model for the material that can more faithfully represent the behaviour of dense sands, for which the accumulated displacement over a particular slip surface leads to a reduction in the friction angle ϕ, until eventually the friction angle reaches a residual value (Muir Wood, 1990). The full model is illustrated in Figure 6c, which also shows the three key material parameters: peak friction angle ϕ_p, residual friction angle ϕ_r, and mobilisation length u_r. In the analysis, each node is assigned a variable that tracks the instantaneous strength ϕ with the accumulated displacement.

Figure 7 directly compares predictions obtained using the numerical model with experimental results. In Figures 7a and 7b, which show the pattern of deformation as it evolves with increasing normalised displacement u/δ, layers of black material were placed in the sand during preparation to show the accumulated deformation, and corresponding lines are shown for the numerical predictions. The red line in the numerical predictions shows the current position of the single slip surface (shear band) assumed in the computational model. The figure reveals that the deformation is characterised by slip surfaces that appear successively at a roughly fixed location relative to the plough rather than moving continuously through the material as assumed in the analytical model (Section 2). This phenomenon is a direct result of softening, which promotes deformation along a single slip surface until the increase in resistance due to material accumulation causes a new slip surface to form in virgin material. As Figures 7a and 7b demonstrate, the numerical model is fully capable of predicting this behaviour, although there is some uncertainty regarding whether the assumed parameters ($\phi_p = 35°$, $\phi_r = 33.5°$, $u_r = 0.1\delta$, and $\phi_w = \phi/3$) are appropriate for the material (Stockton Sand), and whether they would be affected by the method of preparation (tamped), the scale of the experiment ($\delta \approx 100$ mm), the wall roughness (adhered sandpaper), and the relatively narrow width of the apparatus (75 mm). Close inspection of Figures 7a and 7b also reveals zones of localised and continuous shearing near the wall that are not captured by the model. Figure 7c shows that the force-displacement history is also characterised by a succession of jumps corresponding to the changing location of the slip surface. Again, the numerical model predicts the observed response well despite questions regarding which model parameters are most appropriate (see Kashizadeh *et al*. (2014) for details).

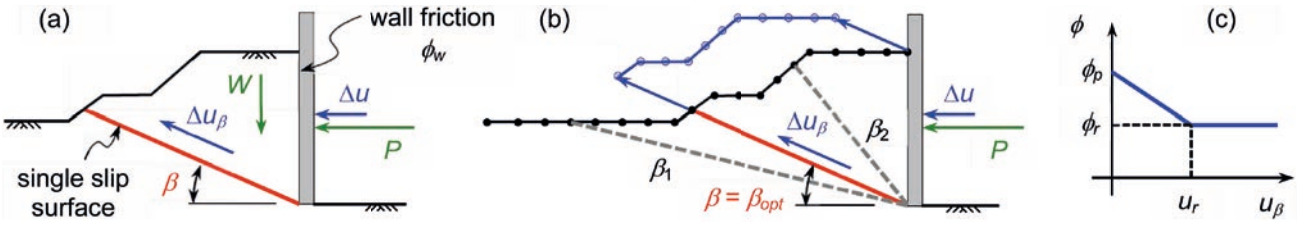

Figure 6: Computational approach for modelling the cutting process in sand: (a) assumed mode of deformation; (b) discretisation, optimisation, and updating; and (c) definition of softening.

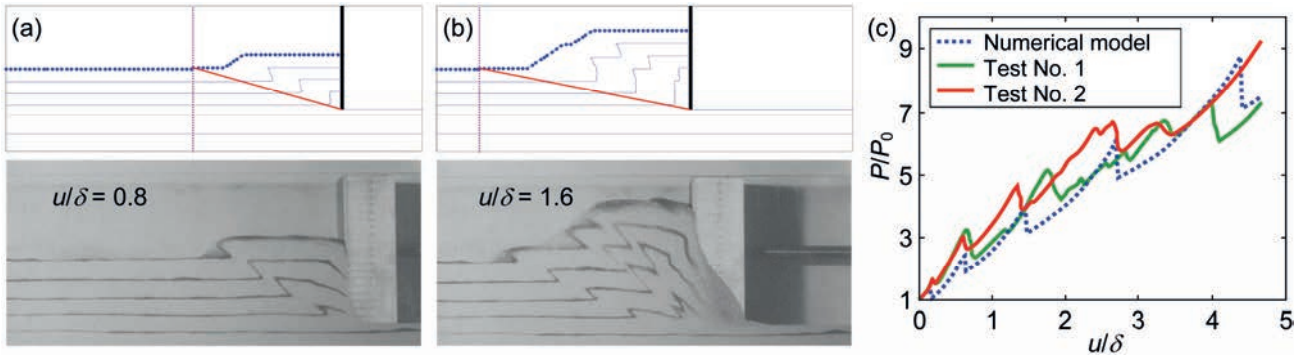

Figure 7: Comparison between numerical and experimental results: (a,b) predicted patterns of deformation compared with images from preliminary 1g experiments conducted at The University of Newcastle using dry Stockton Sand (cf. Rossiter, 2012); (c) predicted force-displacement histories compared with 1g measurements obtained at The University of Western Australia using super fine silica sand (Kashizadeh *et al.*, 2014).

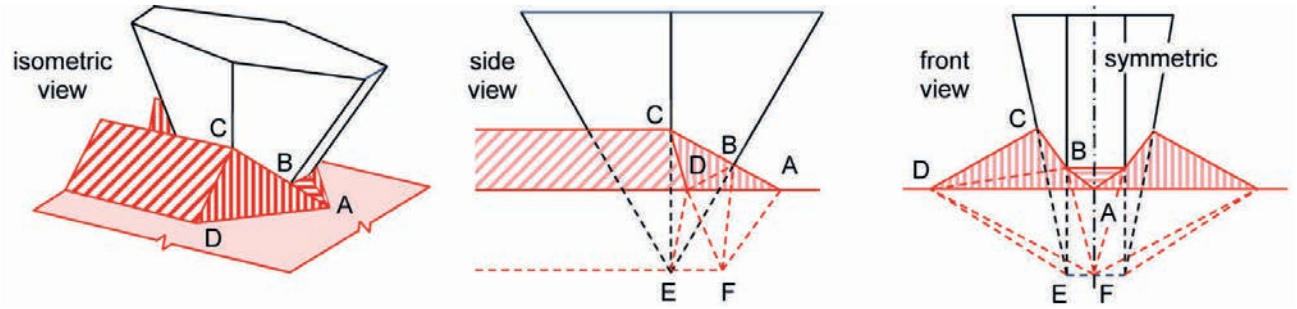

Figure 8: Three-dimensional mode of deformation (adapted from Azarkhin and Devenpeck, 1997).

Future work on the two-dimensional analytical and numerical models will focus on several potential improvements: (1) the introduction of a rich kinematic framework that can account for multiple zones of shearing, including continuous shearing, (2) enhanced constitutive models that account for softening/hardening and dilatancy/compaction in a systematic manner, (3) extension to arbitrary tool configurations (e.g., inclination, shape) and (4) combined lateral and vertical tool motion. A general expression for P, obtained by equating the dissipation rate to the power expended by external forces (energy balance), is

$$P = \frac{1}{\Delta u}\left(\int_V \Delta D dv + \int_{\partial V} \Delta f ds + \int_V \gamma \Delta u_v dv\right) \tag{7}$$

where ΔD is the rate of dissipation by plastic deformation per unit volume (within the deforming volume V), Δf is the rate of dissipation by frictional forces (over the contact surface ∂V), and Δu_v is the vertical component of incremental displacement (positive opposite the direction of gravity). Based on Equation (7) and other constraints required for kinematic admissibility, the optimisation-based finite element framework (e.g., Sloan and Kleeman, 1995; Lyamin and Sloan, 2002) will be utilised to enrich the kinematics.

The proposed approach can also be extended to model three-dimensional ploughing and cutting processes by postulating and subsequently optimising suitable three-dimensional displacement fields. These will be akin to models developed for analysis of friction generated on metallic surfaces due to contacting asperities (e.g., De Vathaire *et al.*, 1981; Azarkhin and Devenpeck, 1997). Figure 8 shows an example in which deformation occurs entirely within planar slip surfaces (shear bands), and the regions bounded by the surfaces translate as rigid blocks. Conceptually, this is a natural extension of the two-dimensional model described above, although the three-dimensional nature of the problem adds considerable complexity to the analysis.

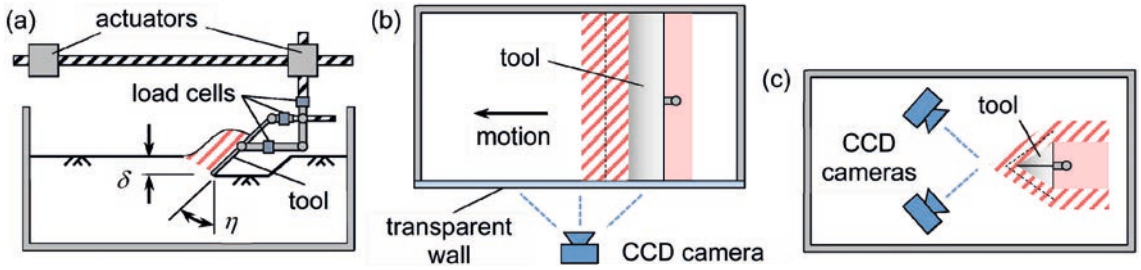

Figure 9: Schematic of experimental setup: (a) side view for two-dimensional (plane strain) tests; (b) plan view for two-dimensional tests; (c) plan view for three-dimensional tests.

4 PHYSICAL MODELLING

A comprehensive experimental programme aimed at validating the proposed theoretical models will be completed using the centrifuge facilities available at the Centre for Offshore Foundations Systems (COFS) at The University of Western Australia. A schematic of the apparatus planned for the physical tests is shown in Figure 9. It consists of a strongbox (500×700×500 mm) containing a soil sample and a model plough or cutting tool. The tool is attached to a system of electric screw actuators controlling horizontal and vertical movement. The assembly is instrumented with customised load cells that can isolate the horizontal and vertical components of force applied to the face of the tool (Figure 9a). As the constitutive behaviour of soils is scale-dependent, a feature manifested most notably in the tendency for localised deformation, variations in the pattern of deformation with the depth δ and displacement u may be significant. In conventional 1g testing, the depth δ and displacement u are limited by geometric constraints on the apparatus. This limitation will be overcome with the aid of the fixed-beam centrifuge at COFS, which enables the prototype dimensions to be varied by orders of magnitude. In the centrifuge, length scales proportionally with n, where n is the g-level within the centrifuge normalised by gravitational acceleration. The tests in the centrifuge will assist in developing scaling relationships based on suitable dimensionless groups, some of which may contain variables not yet recognised as significant.

Tests designed to replicate two-dimensional (plane strain) conditions can be carried out by making the model tool the same width as the strongbox, as shown in Figure 9b. Preliminary tests with a thin, vertical blade have been completed (Kashizadeh *et al*., 2014), but the full series of initial tests will also consider the angle of attack η, shown in Figure 9a. For small depths and large angles of attack, one expects that material will not accumulate on the surface of the plate (cutting), but rather slide over it and eventually reach a steady-state configuration. As the depth increases, or the angle of attack decreases, material will preferentially accumulate ahead of the plate (ploughing) and potentially continue to deform as the displacement u increases. One side of the strongbox is made of Perspex, and the sequence of deformation has been captured via digital images at a high frame rate, using a high resolution CCD camera that captures 5 megapixel images at rates over 10 frames per second. The experiments are expedited by conducting multiple tests on the same soil sample, by carefully removing the deformed layers from the top of the sample and completing subsequent tests in the remainder of the virgin sample (cf. White and Dingle, 2011).

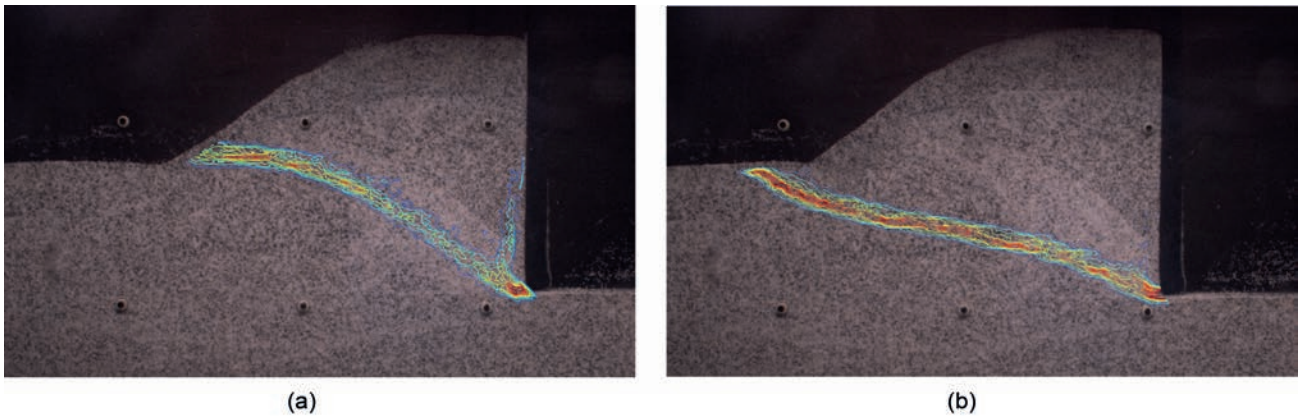

Figure 10: Evolution of failure mechanism for lateral cutting of sand by a vertical blade at 1g (contours show incremental shear strain): (a) steep concave downward failure surface before transition to a (b) new failure surface that is straighter and at smaller inclination from the horizontal.

Data collected from the physical tests will be interpreted and analysed in the following manner. First, the image sequences and force histories will be qualitatively examined to broadly identify and categorise the various patterns of

deformation. Detecting the existence, or lack thereof, of steady, periodic, or pseudo-steady (asymptotic or self-similar) states, as well as the unknown conditions that precipitate these states (Hill, 1950; Petryk, 1979), will be particularly useful in developing the theoretical components. Second, selected image sequences corresponding to characteristic deformation patterns will be analysed using Particle Image Velocimetry (PIV) software (e.g., White *et al*., 2003). This analysis will highlight features that cannot be seen from the images alone, and provide quantitative results which can be compared against the predictions from the numerical models. Figure 10 shows an example of one such analysis, showing the changing inclination and shape of the mobilised failure surface (indicated by incremental shear strain contours) during lateral cutting by a vertical blade. This model test was performed at 1g in dense sand, and the increment of lateral displacement between Figures 10a and 10b was ~5 mm.

As the width of the tool decreases, material preferentially flows to the sides of the tool (ploughing), and the deformation becomes fundamentally three-dimensional. This transition from two dimensions to three dimensions increases the difficulty with respect to quantifying and understanding the pattern of deformation exponentially. Also, a major challenge arises in establishing a thorough testing programme that captures all the essential modes of deformation, due to the enormity of possible variations in the tool's geometry. Methods for evaluating the entire three-dimensional pattern of deformation within a soil mass require sophisticated equipment, and they can be applied only to limited sample sizes and simple loading conditions (Hall *et al*., 2010). One partial visualisation technique is through so-called half-model testing, which relies on placing half of the full model against the Perspex wall and then regarding the soil displacements at the wall as approximations of the displacements at mid-plane in the full 3D configuration (cf. Hambleton and Drescher, 2009). Downsides of this approach include the difficulty in measuring forces and the distortion of the true three-dimensional deformation by wall friction. An alternative that will be considered in future work is to use close-range photogrammetric methods to quantify the overall deformed shape rather than attempt to quantify displacements and strains within the material. By placing two cameras within the strongbox, with fixed control points at known locations within the field of view, synchronous images from two different angles will be obtained over the full process of deformation (Figure 9c).

5 CONCLUDING REMARKS

The paper presents current and future research within the ARC Centre of Excellence for Geotechnical Science and Engineering aimed at understanding and predicting the forces and deformation occurring in ploughing and cutting processes in soils, which lie at the heart of many earthmoving techniques. On account of mining, dredging and construction activities and large investments in infrastructure, earthmoving operations in Australia are among the largest per capita in the world. The research described in this paper is aimed at facilitating technological changes that directly benefit earthmoving operations through potential increases in production rates and improvements in efficiency. By focusing on the particular case of two-dimensional cutting in sand by a vertical blade, the analyses presented in this paper demonstrate the possibility of developing rigorous analytical and numerical models that can account for the progressive nature of the deformation occurring in ploughing and cutting processes. An explicit example of the insights that can be gleaned was given in Section 2, where it was demonstrated that excavation in multiple thin layers may require less energy than excavation in a single thick layer. By establishing and validating a full set of analytical and numerical tools applicable to a range of configurations and soil types, optimal ploughing and cutting configurations for various applications can be recognised.

6 REFERENCES

Atkins, A.G. (2009). *The Science and Engineering of Cutting: The Mechanics and Processes of Separating and Puncturing Biomaterials, Metals and Non-metals*. Butterworth-Heinemann: Amsterdam.

Australian Bureau of Statistics (2011). Australian System of National Accounts 5204.0.

Azarkhin, A., Devenpeck, M. (1997). Enhanced model of a plowing asperity. *Wear*, 206(1-2), 147-155.

Balovnev, V.I. (1983). *New Methods for Calculating Resistance to Cutting of Soil*. English translation from 1963 edition. Amerind: New Delhi.

Chen, W.F. (1975). *Limit Analysis and Soil Plasticity*. Elsevier: Amsterdam.

Cubas, N., Leroy, Y.M., Maillot, B. (2008). Prediction of thrusting sequences in accretionary wedges. *Journal of Geophysical Research*, 113(B12), 1-24.

De Vathaire, M., Delamare, F., Felder, E. (1981). An upper bound model of ploughing by a pyramidal indenter. *Wear*, 66(1), 55-64.

Godwin, R.J., O'Dogherty, M.J. (2007). Integrated soil tillage force prediction models. *Journal of Terramechanics*, 44, 3-14.

Hall, S.A., Bornert, M., Desrues, J., Pannier, Y., Lenoir, N., Viggiani, G., Besuelle, P. Discrete and continuum analysis of localised deformation in sand using X-ray μCT and volumetric digital image correlation. *Géotechnique*, 60(5), 315-322.

Hambleton, J.P., Drescher, A. (2009). Modeling wheel-induced rutting in soils: Rolling. *Journal of Terramechanics*, 46(2), 35-47.

Hambleton, J.P., Drescher, A. (2012). Approximate model for blunt objects indenting cohesive-frictional materials. *International Journal for Numerical and Analytical Methods in Geomechanics*, 36(3), 249-271.

Hill, R. (1950). *The Mathematical Theory of Plasticity*. Oxford University Press: Oxford.

Hooke, R.LeB. (1994). On the efficacy of humans as geomorphic agents. *GSA Today*, 4(9), 217, 224-225.

Hooke, R.LeB. (2000). On the history of humans as geomorphic agents. *Geology*, 28, 843-846.

Kashizadeh, E., Hambleton, J.P., Stanier, S.A. (2014). A numerical approach for modelling the ploughing process in sands. *Proc. 14th International Conference of the International Association for Computer Methods and Advances in Geomechanics*, Kyoto, Japan, Sept. 22-25, (accepted).

Knappett, J.A., Brown, M.J., Bransby, M.F., Hudacsek, P., Morgan, N., Cathies, D., Maconochie, A., Yun, G., Ripley, A.G., Brown, N., and Egborge, R. (2012). Capacity of grillage foundations under horizontal loading. *Géotechnique*, 62(9), 811-823.

Lyamin, A.V., Sloan S.W. (2002). Upper bound limit analysis using linear finite elements and non-linear programming. *International Journal for Numerical and Analytical Methods in Geomechanics*, 26(2), 181-216.

McKyes, E. (1985). *Soil Cutting and Tillage*. Elsevier: Amsterdam.

Muir Wood, D. (1990). *Soil Behaviour and Critical State Soil Mechanics*. Cambridge University Press: Cambridge.

Palmer, A.C. (1999). Speed effects in cutting and ploughing. *Géotechnique*, 49(3), 285-294.

Petryk, H. (1979). On slip-line field solutions for steady-state and self-similar problems with stress-free boundaries. *Archives of Mechanics*, 31(6), 861-74.

Rossiter, T.R. (2012). *Analysis of the Ploughing Process in Dry Sand*. Final-year project report. University of Newcastle: Newcastle.

Sloan S.W., Kleeman, P.W. (1995). Upper bound limit analysis using discontinuous velocity fields. *Computer Methods in Applied Mechanics and Engineering*, 127(1-4), 293-314.

Sutoh, M., Nagaoka, K., Nagatani, K., Yoshida, K. (2013). Design of wheels with grousers for planetary rovers traveling over loose soils. *Journal of Terramechanics*, 50(5-6), 345-353.

Terzaghi, K. (1943). *Theoretical Soil Mechanics*. John Wiley and Sons: New York.

White, D.J., Dingle, H.R.C. (2011). The mechanism of steady friction between seabed pipelines and clay soils. *Géotechnique*, 61(12), 1035-1041.

White, D.J., Take, W.A., Bolton, M.D. (2003). Soil deformation measurement using particle image velocimetry (PIV) and photogrammetry. *Géotechnique*, 53(7), 619-731.

Wilkinson, A., DeGennaro, A. (2007). Digging and pushing lunar regolith: Classical soil mechanics and the forces needed for excavation and traction. *Journal of Terramechanics*, 44(2), 133-152.

Yang, W.H. (1993). Large deformation of structures by sequential limit analysis. *International Journal of Solids and Structures*, 30(7), 1001-1013.